

Plastic zone at crack tip: A nanolab for formation and study of metallic glassy nanostructures

Xing-Xiang Xia and Wei-Hua Wang^{a)}

Institute of Physics, Chinese Academy of Sciences, Beijing 100080, People's Republic of China

A. Lindsay Greer

Department of Materials Science and Metallurgy, University of Cambridge, Cambridge CB2 3QZ, United Kingdom

(Received 11 November 2008; accepted 20 March 2009)

We report that various metallic glassy nanostructures including nanoridges, nanocones, nanowires, nanospheres, and nanoscale-stripped patterns are spontaneously formed on the fracture surface of bulk metallic glasses at room temperature. A clear correlation between the dimensions of these nanostructures and the size of the plastic zone at the crack tip has been found, providing a way to control nanostructure sizes by controlling the plastic zone size intrinsically or extrinsically. This approach to forming metallic glassy nanostructures also has implications for understanding the deformation and fracture mechanisms of metallic glasses.

I. INTRODUCTION

Novel system performance through nanostructuring has been investigated in many branches of science in recent years.¹ One of the most active trends in this field is the development of synthetic methods to obtain shape- and size-controlled nanostructures, because various behaviors of these nanostructures such as physical and chemical properties^{2,3} are strikingly sensitive to both morphology and size. The categories of metallic alloys and metal oxide nanostructures are important and have been extensively studied due to their scientific interest and practical applications. However, most of these metallic nanostructures are crystalline,^{4,5} despite the fact that the superiority of the amorphous over the nanocrystalline state has been demonstrated in some cases such as chemical catalysis.⁶ More recently, it has been predicted theoretically^{7–9} and confirmed experimentally^{6,10} that the amorphous state is naturally favorable and feasible for stable nanostructures.

Bulk metallic glasses (BMGs), exhibiting unique physical, chemical (such as high resistance to corrosion and oxidation), and mechanical (such as extraordinarily high strength, hardness, and elastic limit) properties, have attracted extensive attention because of their potential for engineering application and their scientific interest.¹¹ In contrast to dislocation-mediated plastic flow in crystalline metallic alloys, BMGs normally display little global plasticity before fracture because their plastic deformation at room temperature is highly localized in nanoscale shear

bands, where a large plastic strain is accumulated in a very thin region (10–20-nm thick) exhibiting strain softening or thermal softening.¹² The softening leads to the formation of a viscous fluid-like layer that manifests itself in remarkable patterns when the shear band comes apart in final fracture (for a review see Ref. 12).

Using the unique nature of the localized plasticity of BMGs, in this letter, we report a consequence of the local plastic behavior, namely spontaneous formation of a family of metallic glassy nanostructures including nanoridges, nanocones, nanowires, nanospheres, and nanoscale periodic striations by simply fracturing BMGs at room temperature. Because of the original metallic glass state and the extremely high cooling rate in the plastic zone at the crack tip during fracture, the formed nanostructures are also in the glassy state. The dimensions of the nanostructures can be controlled by controlling the size of the plastic zone of BMGs intrinsically or extrinsically.

II. EXPERIMENTAL

The BMGs were prepared by standard methods: arc melting the pure elements under Ar atmosphere and then suction-casting into a Cu mold to give cylindrical samples, 3 mm in diameter and 20 mm in length. A diamond saw was used to introduce a notch (1.5 mm wide and 200 μm deep) in the middle of one side of the cylinders. Fresh fracture surfaces were obtained by conventional three-point bend-testing on an Instron 4505 machine (Norwood, MA) with a constant displacement velocity of 0.5 mm/min at room temperature. The amorphous nature of the samples and of their fresh fracture surfaces was confirmed by x-ray diffraction,

^{a)}Address all correspondence to this author.

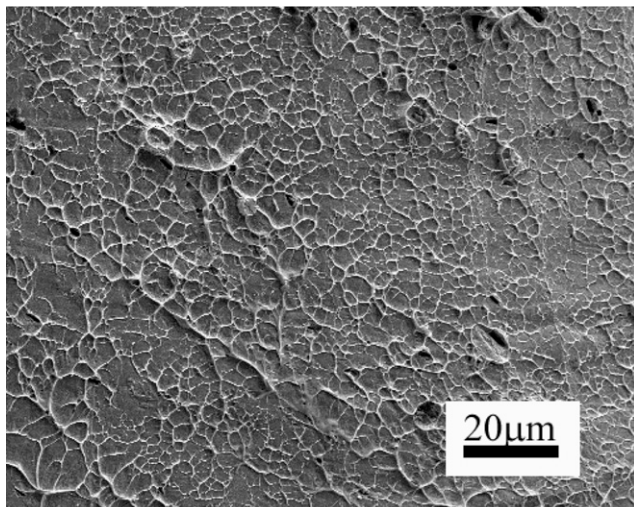
e-mail: whw@aphy.iphy.ac.cn

DOI: 10.1557/JMR.2009.0362

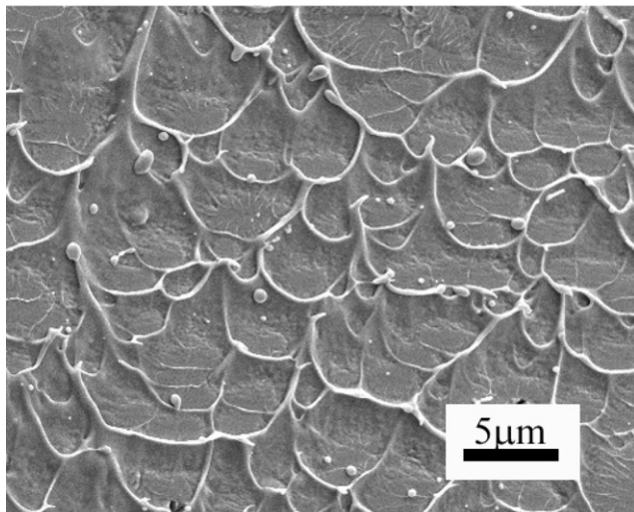
and the nanostructures on fresh fracture surfaces were observed using scanning electron microscopy (SEM; Philips XL30 instrument; Eindhoven, The Netherlands).

III. RESULTS AND DISCUSSIONS

Figure 1(a) shows an SEM picture at low magnification of the fracture surface, near the notch, of a $\text{Ce}_{70}\text{Al}_{10}\text{Cu}_{10}\text{Ni}_{10}$ BMG that has excellent glass-forming ability, exceptionally low glass transition temperature T_g , and high thermodynamic and kinetic stability.¹³ The fracture surface is predominantly characterized by nanoridges (appearing white), which form a typical vein pattern on the relatively smooth crack plane. However, at higher magnification [Fig. 1(b)] it can be seen that many spheres or droplets, ranging from tens to hundreds of nanometers in diameter, are distributed between the



(a)



(b)

FIG. 1. (a) Typical vein pattern on the fracture surface of Ce-based BMG. (b) Higher magnification showing nanospheres between the veins.

veins. The presence of these nanospheres reveals that the local temperature during fracture was sufficiently high compared with T_g that the local viscosity had decreased to give liquid-like behavior. Similar heating is known to occur at shear bands.^{14,15}

With further observation, one can find various morphologies of nanostructures including nanoridges, nanoridges, nanowires, and nanospheres on the fracture surface of this Ce-based BMG. Figure 2(a) shows clearly a portion of a nanoridge with an approximately triangular cross-section ~ 250 nm wide at the base and ~ 350 nm high. When nanoridges meet, a nanocone can be readily found in the vicinity of the intersection. Figure 2(b) represents such a nanoscale cone with a symmetrical profile and oriented nearly perpendicular to the crack plane. Such configurations clearly show that on the nanoscale the fracture of BMGs is ductile, with peak-to-peak separation analogous to the completely ductile fracture of polycrystals.^{16,17} Some nanowires can also be found formed from similar intersections. In Fig. 2(c), a uniform nanowire ~ 340 nm in diameter and ~ 19.6 μm in length is attached on the fracture surface. In close-up [inset of Fig. 2(c)], the nanowire is remarkably uniform, implying that viscous flow has readily occurred during its formation. Adjacent to the nanowires many spheres ranging from tens to hundreds of nanometers in diameter can again be found; the example in Fig. 2(d) has a diameter of ~ 180 nm. In other brittle BMGs, such as Mg-based BMGs, nanoscale striped patterns with a spacing of ~ 70 nm¹⁷ have been observed on fracture surface [Figs. 2(e) and 2(f)].

In standard fracture mechanics, it is accepted that there is a well defined plastic zone at the crack tip as shown in Fig. 3(a) (top). The plastic zone size l_p for BMGs for crack propagation under plane strain can be expressed approximately as^{16,18}: $l_p = 0.025(K_c/\sigma_y)^2$, where the fracture toughness K_c ¹⁹ and yield stress σ_y for the Ce-based BMG are $10 \text{ MPa m}^{0.5}$ and 650 MPa , respectively.¹⁶ The typical vein size w and plastic zone size l_p for a broad range of BMGs have been confirmed experimentally to scale, with $w \approx l_p$.¹⁶ The calculated l_p of the Ce-based BMG is approximately $6.0 \mu\text{m}$ and fits well with the dimple size [Fig. 1(b)]. The maximum temperature rise in the narrow plastic zone associated with a moving crack is given by²⁰:

$$\Delta T = \sqrt{2} \frac{(1 - \nu^2) K_c \sigma_y \sqrt{V}}{E \sqrt{\rho \kappa c}}, \quad (1)$$

where the Poisson ratio ν , Young modulus E , density ρ , specific heat c , and thermal conductivity κ for the Ce-based BMG are 0.313 , 30.3 GPa , 6.67 g cm^{-3} , $1 \text{ J g}^{-1} \text{ K}^{-1}$, and $5 \text{ W m}^{-1} \text{ K}^{-1}$, respectively.^{13,18} The maximum crack velocity V is typically $\sim 0.5 V_R$ for brittle materials, and the Rayleigh wave velocity

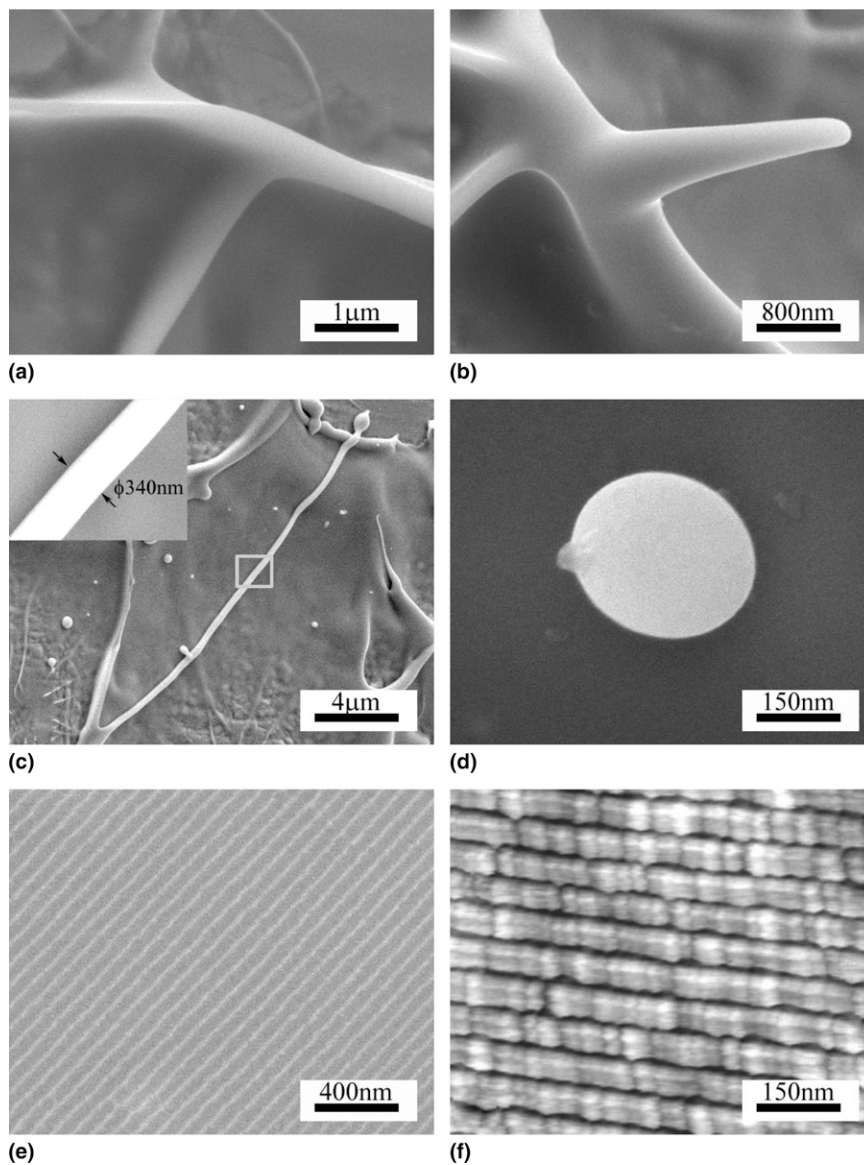


FIG. 2. (a)–(d) Fine nanostructures on the fracture surface of Ce-based BMG: (a) a portion of a nanoridge constituting the typical vein pattern; (b) a nanocone in the vicinity of a ridge intersection; (c) a uniform nanowire with a diameter of 340 nm; (d) a nanosphere with a diameter of 180 nm; (e) SEM image; and (f) atomic-force-microscope image of a nanoscale-striped pattern with a spacing of ~ 70 nm on the fracture surface of Mg-based BMG.

$V_R \approx 0.9 V_S$. For the Ce-based BMG, the shear wave velocity V_S is 1315 m s^{-1} ¹³ and finally the crack velocity is estimated to be 500 m s^{-1} . Thus, the maximum temperature rise ΔT in plastic zone can instantaneously reach up to $\sim 1000 \text{ K}$, which fits with experimental observations on shear bands.¹⁴ Flores and Dauskardt²¹ previously used Eq. (2) to calculate the temperature rise at a moving crack tip in a BMG, but they assumed a much lower crack velocity ($< 0.2 \text{ m s}^{-1}$) and correspondingly estimated a temperature rise of a few tens of degrees that would not agree with observations of liquid-like behavior.

High temperatures in the plastic zone rapidly decrease through heat conduction to the surrounding bulk. The

crack tip acts as an instantaneous line source of heat. The two-dimensional temperature distribution around the line a time t after the heating is given by^{21,22}:

$$\Delta T = \frac{q}{4\pi\kappa t} \exp\left(\frac{-r^2}{4\alpha t}\right), \quad (2)$$

where q is the heat content of the line source [estimated from Eq. (1) to be 0.15 J m^{-1}], r is the radial distance from the line, and α is the thermal diffusivity ($\sim 10^{-6} \text{ m}^2 \text{ s}^{-1}$). Taking $r = 0.5 l_p$ and a ΔT corresponding to heating up to T_g (360 K for the Ce-based BMG), and this is the cooling rate relevant for glass formation. The cooling rate estimated from Eq. (3) is $\sim 2 \times 10^6 \text{ K s}^{-1}$. Of course, this rate may be altered when the crack surfaces part on

fracture. Nevertheless, the cooling rate greatly exceeds the critical cooling rate for glass formation (10^2 K s^{-1} for the Ce-based BMG¹³) and ensures the glassy structure¹⁰ of the nanostructures formed in the plastic zone.

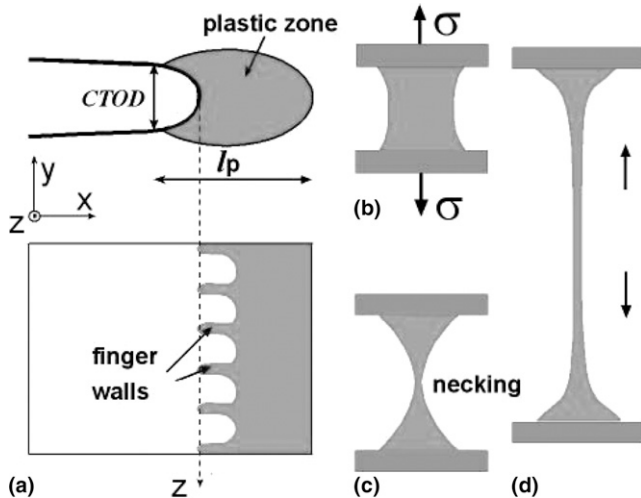


FIG. 3. (a) Schematic of the plastic zone at a crack tip. The top shows a cross-section of the crack, and the bottom shows a plan view of the plastic zone in which a viscous fingering pattern emerges due to the meniscus instability. The crack opening and the fingering pattern are exaggerated. A viscous bridge (b) from a finger wall subjected to tension can (c) lead to cones through two-dimensional necking of the bridge, or (d) to a nanowire through superplastic flow of the bridge.

The intense shear rate immediately at the crack tip can be estimated from $\dot{\gamma} = V/CTOD$. The crack tip opening displacement (CTOD) can be expressed as²³: $CTOD = 24\sqrt{3}\pi^2 B(n)\chi/\sigma_y$, where the surface energy χ and dimensionless parameter $B(n)$ are 1 J m^{-2} and 1.2, respectively. The CTOD is $\sim 800 \text{ nm}$ and the shear rate approaches $\sim 10^8 \text{ s}^{-1}$. Consequently, the nanoscale plastic zone at the crack tip experiences conditions of high temperature, high cooling rate, and high shear rate.

This nanoscale plastic zone offers a natural “laboratory” for formation of metallic nanostructures. The extreme physical conditions inside the zone guarantee the glassy state of the formed nanostructures. As the crack advances into the plastic zone with much reduced viscosity, a viscous fingering pattern [Fig. 3(a)] appears at the crack tip due to the meniscus instability. The finger walls act as discontinuous viscous bridges and undergo plastic deformation via a one-dimensional necking process under tensile stress, leading to tapered nanoridges, wide at the base and sharp at the top [Fig. 2(a)]. If these nanoridges meet, the situation is more complicated and a cylindrical liquid bridge emerges [Fig. 3(b)]. The necking of nanoscale BMG samples under tensile stress has been clearly examined in situ with TEM at room temperature,²⁴ and the viscous bridges here can simply be considered as series of nanoscale BMG samples. Plastic deformation of a cylindrical liquid-like bridge under tension can lead to necking [Fig. 3(c)] and the formation of

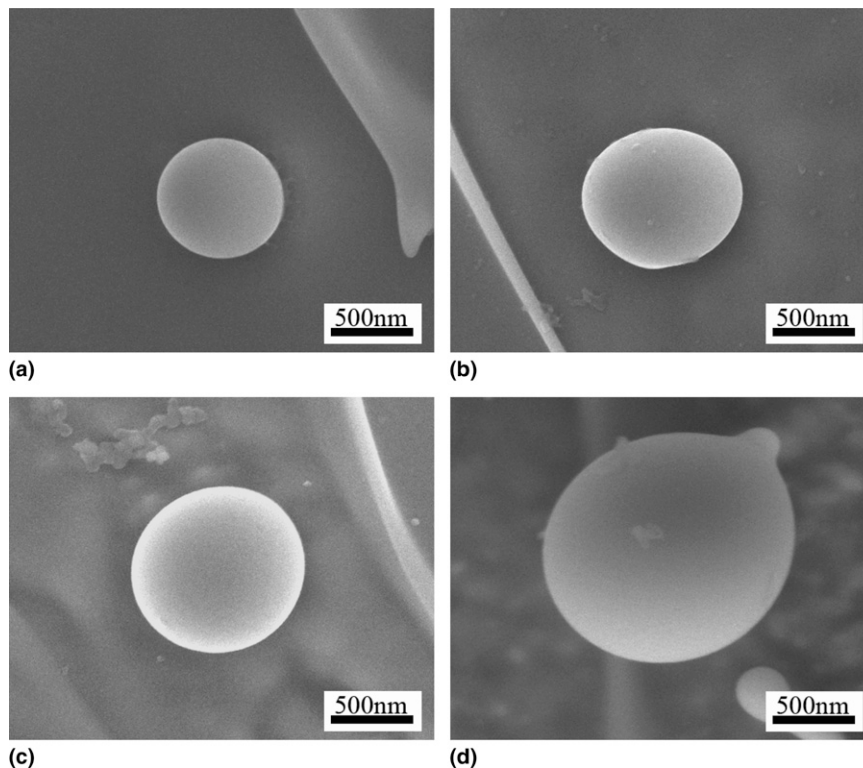


FIG. 4. SEM images of the characteristic largest nanospheres for a variety of typical BMGs fractured under the same condition. (a) Ce-based, (b) $\text{Zr}_{57}\text{Cu}_{15.4}\text{Ni}_{12.6}\text{Al}_{10}\text{Nb}_5$, (c) Cu-based, and (d) $\text{Zr}_{41.2}\text{Ti}_{13.8}\text{Cu}_{12.5}\text{Ni}_{10}\text{Be}_{22.5}$.

two well-aligned nanocones [Fig. 2(b)]. Alternatively, with suitable local viscosity and strain rate, the cylindrical liquid-like bridge behaves in a superplastic manner²⁵ and can be stretched uniformly thousands of percent without necking [Fig. 3(c)]. The nanowires formed on the present fracture surfaces likely form under a load-controlled-like mechanism, very similar to the macro experiments showing macro/microwire formation as shown by Vormelker et al.²⁶ The viscous bridge model [Figs. 3(b) and 3(d)] allows us to estimate the local elongation of the nanowire in Fig. 2(c). The original length of the bridge can be considered as the CTOD, and its value (~ 800 nm) is well consistent with $2h$, where h is the height of the nanoridge [350 nm in Fig. 2(a)]. Thus, the local elongation can be calculated as follows: length/CTOD $\gg 2500\%$. In addition, if the local viscosity is too low or the local strain rate is too high, the deformation and final rupture of the viscous materials in plastic zone break up the viscous bridges and, through a Rayleigh instability, can give rise to some individual spheres.

These nanostructures with different length scales have also been found on fracture surfaces of other BMGs with markedly different compositions and mechanical properties. Figure 4 shows characteristic nanospheres on fracture surfaces for a variety of typical BMGs. For simplicity, only the largest spheres for a specific BMG have been considered. The size of the nanospheres is clearly very different for different BMG systems. Recent studies have demonstrated that the vein size on fracture surfaces also takes characteristic values for different BMGs.¹⁶ For a wide range of BMGs, Figs. 5(a) and 5(b) show the clear relationships between the average largest sphere diameter D , the average width of the nanoridges W , and the vein size w ; the relevant values are given in Table I. The experimental data on D , W , and w have been obtained either from the SEM observations of fracture surfaces or directly from the literature. The nanoridge width measured here is in good agreement with the typical value of 100 to 200 nm.³⁰ The results indicate that both D and W curves have a similar shape and the values generally increase with increasing w . It is

useful to link the dimensions of the nanostructures (i.e., D and W) to w , because the value of w can be determined from the fracture toughness and yield stress of a BMG.¹⁶ This physical constraint/modification can be readily rationalized because the formation of these structures is ascribed to plastic flow in the zone at the crack tip. Intrinsically, the plastic zone size l_p of the as-cast BMGs ranges broadly from ~ 1 mm for tough Zr-based BMGs down to ~ 10 nm for typically brittle Fe-based BMGs.^{11,27} The clear correlation between the mechanical behavior of BMGs (K_C and σ_y) and the nanostructure dimensions assists in approximately controlling the size of the nanostructures spontaneously formed by

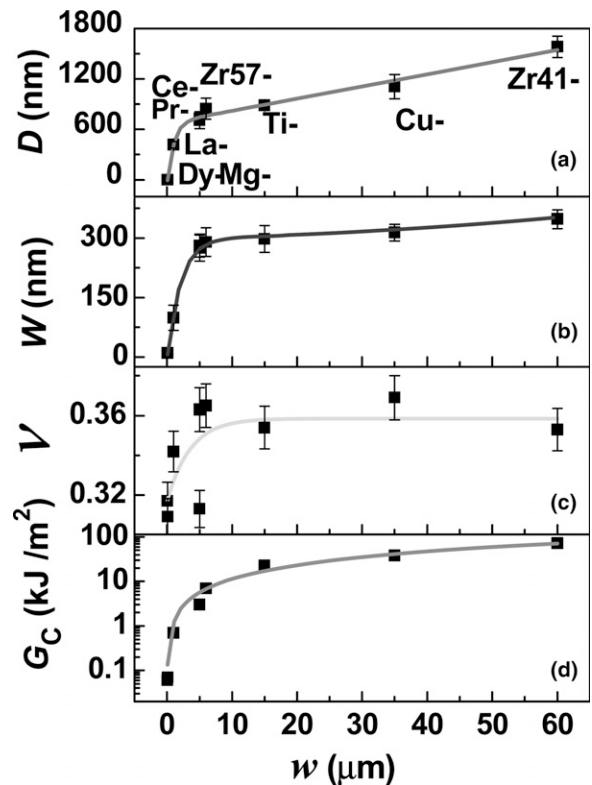


FIG. 5. (a) Dependences of the average diameter of the largest spheres D , (b) the width of nanoridges W , (c) Poisson ratio ν , and (d) fracture energy G_C on typical vein size w on the same fracture surface for a range of BMGs.^{16,17,27–29}

TABLE I. The parameters of vein size (w), the average diameter of the largest spheres (D), width of nanoridge (W), elastic modulus ratio (μ/B), Poisson ratio (ν), and fracture energy (G_C) of a range of typical BMGs.

BMGs	w (μm)	D (nm)	W (nm)	μ/B	ν	G_C (kJ m^{-2})	Refs.
Dy ₄₀ Y ₁₆ Al ₂₄ Co ₂₀	0.08		10	0.417	0.317	0.06	17
Mg ₆₅ Cu ₂₅ Tb ₁₀	0.1		10	0.439	0.309	0.07	16, 27
La ₅₅ Al ₂₅ Cu ₁₀ Ni ₅ Co ₅	1	417 \pm 39	99 \pm 32	0.354	0.342	0.7	28
Pr ₆₀ Al ₁₀ Ni ₁₀ Cu ₂₀	5	709 \pm 100	281 \pm 29	0.302	0.363		27
Ce ₇₀ Al ₁₀ Cu ₁₀ Ni ₁₀	5	731 \pm 60	275 \pm 33	0.427	0.313	3	16, 27
Zr ₅₇ Cu _{15.4} Ni _{12.6} Al ₁₀ Nb ₅	6	848 \pm 127	290 \pm 36	0.297	0.365	7	27
Ti ₄₀ Zr ₂₅ Ni ₃ Cu ₁₂ Be ₂₀	15	886 \pm 58	298 \pm 34	0.324	0.354	22.74	16, 29
Cu ₆₀ Zr ₂₀ Hf ₁₀ Ti ₁₀	35	1110 \pm 145	314 \pm 21	0.288	0.369	38	16, 27
Zr _{41.2} Ti _{13.8} Cu _{12.5} Ni ₁₀ Be _{22.5}	60	1583 \pm 128	348 \pm 24	0.324	0.353	72	16, 27

fracture of appropriate BMG systems through the different sizes of the plastic zone. The plastic zone size can also be tuned by gradually changing the mechanical properties of BMGs through extrinsic methods such as annealing^{27,31} and, in turn, can control the size of the nanostructures. The toughness K_C of BMGs, or alternatively the fracture energy G_C , has been found to correlate with the Poisson ratio ν (or with the ratio of elastic shear modulus μ and the bulk modulus B).^{27,32–34} From Figs. 5(c)–5(d) one can see a clear correlation between w and G_C (or ν). The correlations of w , mechanical behavior, and ν also assist in understanding flow and fracture mechanisms, and in guiding alloy design to alleviate the macroscopic brittleness of metallic glasses.

IV. SUMMARY

The reported spontaneous formation of various nanoscale structures, with tunable size, in metallic glass is obtained simply by fracturing a metallic glass rod. This facile technique opens up a new avenue for fabrication of amorphous metallic nanoscale structures with high strength and high corrosion resistance, which might be applicable and provide building blocks for the development of small devices. The fabrication of these metallic glassy nanostructures may extend the investigative domain of nanostructure science and technology. For example, a great challenge is assembling and positioning nanoparticles or nanowires in desired locations to construct complex, higher-order functional structures. Controlled positioning of nanoparticles or nanowires has been achieved on predefined templates fabricated by top-down approaches. The spontaneous formation of nanoscale metallic glass-stripped patterns obtained by simply fracturing a metallic glass rod has various applications such as nanoscale gratings or ultraminiaturized integrated circuits. The nanostructure formation also further confirms that there is nanoscale local softening during the fracture of BMGs.¹⁶

ACKNOWLEDGMENTS

We acknowledge the financial support from the National Science Foundation of China (Grant Nos. 50621061 and 50731008) and the National Basic Research Program of China (MOST 973; Grant No. 2007CB613904).

REFERENCES

1. J.R. Heath: Nanoscale materials. *Acc. Chem. Res.* **32**, 388 (1999).
2. J. Bosbach: Ultrafast dephasing of surface plasmon excitation in silver nanoparticles: Influence of particle size, shape, and chemical surrounding. *Phys. Rev. Lett.* **89**, 257404 (2002).
3. C.R. Martin: Nanomaterials: A membrane-based synthetic approach. *Science* **266**, 1961 (1994).
4. T.S. Ahmadi, Z.L. Wang, T.C. Green, A. Henglein, and M.A. El-Sayed: Shape-controlled synthesis of colloidal platinum nanoparticles. *Science* **272**, 1924 (1996).
5. Y.M. Wang, M.W. Chen, F.H. Zhou, and E. Ma: High tensile ductility in a nanostructured metal. *Nature* **419**, 912 (2002).
6. K.S. Suslick, S.B. Choe, A.A. Cichowlas, and M.W. Grinstaff: Sonochemical synthesis of amorphous iron. *Nature* **353**, 414 (1991).
7. H. Ikeda, Y. Qi, T. Çagin, K. Samwer, W.L. Johnson, and W.A. Goddard III: Strain rate induced amorphization in metallic nanowires. *Phys. Rev. Lett.* **82**, 2900 (1999).
8. S.J.A. Koh, H.P. Lee, C. Lu, and Q.H. Cheng: Molecular dynamics simulation of a solid platinum nanowire under uniaxial tensile strain: Temperature and strain-rate effects. *Phys. Rev. B: Condens. Matter* **72**, 085414 (2005).
9. D.X. Wang, J.W. Zhao, S. Hu, X. Yin, S. Liang, Y.H. Liu, and S.Y. Deng: Where, and how, does a nanowire break? *Nano Lett.* **7**, 1208 (2007).
10. K.S. Nakayama, Y. Yokoyama, G. Xie, Q.S. Zhang, M.W. Chen, T. Sakurai, and A. Inoue: Metallic glass nanowire. *Nano Lett.* **8**, 516 (2008).
11. M.F. Ashby and A.L. Greer: Metallic glasses as structural materials. *Scr. Mater.* **54**, 321 (2006).
12. C.A. Schuh, T.C. Hufnagel, and U. Ramamurty: Mechanical behavior of amorphous alloys. *Acta Mater.* **55**, 4067 (2007).
13. B. Zhang, D.Q. Zhao, M.X. Pan, W.H. Wang, and A.L. Greer: Amorphous metallic plastic. *Phys. Rev. Lett.* **94**, 205502 (2005).
14. J.J. Lewandowski and A.L. Greer: Temperature rise at shear bands in metallic glasses. *Nat. Mater.* **5**, 15 (2006).
15. Y. Zhang, N.A. Stelmashenko, Z.H. Barber, W.H. Wang, J.J. Lewandowski, and A.L. Greer: Local temperature rises during mechanical testing of metallic glasses. *J. Mater. Res.* **22**, 419 (2007).
16. X.K. Xi, D.Q. Zhao, M.X. Pan, W.H. Wang, Y. Wu, and J.J. Lewandowski: Fracture of brittle metallic glasses: Brittleness or plasticity. *Phys. Rev. Lett.* **94**, 125510 (2005).
17. G. Wang, D.Q. Zhao, H.Y. Bai, M.X. Pan, A.L. Xia, B.S. Han, X.K. Xi, Y. Wu, and W.H. Wang: Nanoscale periodic morphologies on the fracture surface of brittle metallic glasses. *Phys. Rev. Lett.* **98**, 235501 (2007).
18. H.L. Ewalds and R.J.H. Wanhill: *Fracture Mechanics* (Edward Arnold, London, 1984), pp. 56–63.
19. P. Lowhaphandu and J.J. Lewandowski: Fracture toughness and notched toughness of bulk amorphous alloy: Zr-Ti-Ni-Cu-Be. *Scr. Mater.* **38**, 1811 (1998).
20. A.S. Argon: *The Physics of Strength and Plasticity* (MIT Press, Cambridge, MA, 1969), p. 286.
21. K.M. Flores and R.H. Dauskardt: Local heating associated with crack tip plasticity in Zr-Ti-Ni-Cu-Be bulk amorphous metals. *J. Mater. Res.* **14**, 638 (1999).
22. H.S. Carslaw and J.C. Jaeger: *Conduction of Heat in Solids*, 2nd ed. (Clarendon Press, Oxford, UK, 1959), pp. 256–258.
23. A.S. Argon and M. Salama: The mechanism of fracture in glassy materials capable of some inelastic deformation. *Mater. Sci. Eng.* **23**, 219 (1976).
24. H. Guo, P.F. Yan, Y.B. Wang, J. Tan, Z.F. Zhang, M.L. Sui, and E. Ma: Tensile ductility and necking of metallic glass. *Nat. Mater.* **6**, 735 (2007).
25. A. Inoue: Stabilization and high strain-rate superplasticity of metallic supercooled liquid. *Mater. Sci. Eng., A* **267**, 171 (1999).
26. A.H. Vormelker, O.L. Vatamanu, L. Kecskes, and J.J. Lewandowski: Effects of test temperature and loading conditions on the tensile properties of a Zr-based bulk metallic glass. *Mater. Trans. A* **39**, 1922 (2008).

27. J.J. Lewandowski, W.H. Wang, and A.L. Greer: Intrinsic plasticity or brittleness of metallic glasses. *Philos. Mag. Lett.* **85**, 77 (2005).
28. J.J. Lewandowski, M. Shazly, and A.S. Nouri: Intrinsic and extrinsic toughening of metallic glasses. *Scr. Mater.* **54**, 337 (2006).
29. F.Q. Guo, H.J. Wang, S.J. Poon, and G.J. Shiflet: Ductile titanium-based glassy alloy ingots. *Appl. Phys. Lett.* **86**, 091907 (2005).
30. D.M. Kulawansa, J.T. Dickinson, S.C. Langford, and Y. Watanabe: Scanning tunneling microscope observations of metallic glass fracture surfaces. *J. Mater. Res.* **8**, 2543 (1993).
31. J.J. Lewandowski: Effects of annealing and changes in stress state on fracture toughness of bulk metallic glass. *Mater. Trans., JIM* **42**, 633 (2001).
32. J. Schroers and W.L. Johnson: Ductile bulk metallic glass. *Phys. Rev. Lett.* **93**, 255506 (2004).
33. X.J. Gu, A.G. McDermott, S.J. Poon, and G.J. Shiflet: Critical Poisson's ratio for plasticity in Fe-Mo-C-B-Ln bulk amorphous steel. *Appl. Phys. Lett.* **88**, 211905 (2006).
34. W.H. Wang: The correlation between the elastic constants and properties in bulk metallic glasses. *J. Appl. Phys.* **99**, 093506 (2006).